Proceedings of AJTEC2011
ASME/JSME 2011 8th Thermal Engineering Joint Conference
March 14-17, 2011, Honolulu, Hawaii, USA

AJTEC2011-44555

EXPERIMENTAL ANALYSIS OF THE SINGLE-PHASE HEAT TRANSFER AND FRICTION FACTOR INSIDE THE HORIZONTAL INTERNALLY MICRO-FIN TUBE

Hou Kuan Tam
Department of Electromechanical Engineering, Faculty of Science and Technology, University of Macau, Av. Padre Tomás Pereira, Taipa, Macau, China.

Lap Mou Tam
Department of Electromechanical Engineering, Faculty of Science and Technology, University of Macau, Av. Padre Tomás Pereira, Taipa, Macau, China.
Institute for the Development and Quality, Macau.

Afshin J. Ghajar
School of Mechanical and Aerospace Engineering, Oklahoma State University, Stillwater, Oklahoma, USA.

ABSTRACT

To increase heat transfer, internally micro-fin tubes are widely used in commercial HVAC applications such as flooded evaporators. It is commonly understood that the micro-fin enhances heat transfer but at the same time increases the pressure drop as well. In the previous studies, majority of the works were focused on the development of correlations in a particular flow regime, especially in the turbulent region. There are only a few works that fundamentally studied the continuous change in the characteristic behavior of heat transfer and pressure drop from laminar to transition and eventually the turbulent regions. Therefore, more in-depth study is necessary. In this study, heat transfer and pressure drop were measured simultaneously in a single test section fitted with 2 micro-fin tubes and compared with the data of a plain tube. From the results, the transition from laminar to turbulent was clearly established. The buoyancy effect is present in the laminar region. The transition from laminar to turbulent was found to be inlet dependent. It could be seen that the delay of transition was more obvious for smaller spiral angle while it was not as obvious when large spiral angle tube was used. Furthermore, it was observed that the larger spiral angle had an enhancement of the heat transfer in the upper transition to turbulent regions. Finally, the efficiency index (the ratio of the heat transfer and the friction factor of enhanced tube to those variables for the plain tube) was examined and it was found to have a value larger than one when Reynolds number is larger than 5000 regardless of the type of inlet configuration used. Therefore, the application of the micro-fin tubes used in this study is suitable when Reynolds number is larger than 5000.

INTRODUCTION

Single-phase liquid flow in internally enhanced tubes is becoming more important in commercial HVAC applications, where enhanced tube bundles are used in flooded evaporators and shell-side condensers to increase heat transfer. This enables water chillers to reach high efficiency, which helps mitigate global warming concerns of HVAC systems. One kind of internally enhanced tube is the micro-fin tube. Jensen and Vlakancic (1999) defined the micro-fin tube to have a height less than $0.03d_i$ (i.e. $2e/d_i<0.06$), where d_i is the inside tube diameter and e is the fin height. Basically, such kind of tube is widely used in high flow rate applications because the heat transfer enhancement in high flow rates (turbulent region) is more pronounced than that in the low flow rates (laminar region). Khanpara et al. (1986) reported that the turbulent heat transfer in micro-fin tubes had an increase of 30 to 100% with Reynolds numbers between 5,000 and 11,000. Brognaux et al. (1997) indicated that there was a 65 to 95% increase in heat transfer for the micro-fin tube over the smooth tube. However, there was also a 35 to 80% increase in the isothermal pressure drop. The work of Jensen and Vlakancic (1999) indicated that the micro-fins increased heat transfer ranging from 20 to 220% in the turbulent flow region. However, there was a penalty due to the increment of friction factor ranging from 40 to 140%. Webb et al. (2000) calculated the "efficiency index", defined as

the ratio of the heat transfer and the friction factor of enhanced tube to those variables for the plain tube, to vary from 0.98 to 1.18 for the seven different micro-fin tubes with Reynolds numbers between 20,000 and 80,000. For the laminar flow, several researchers (Brognaux et al., 1997, Esen et al., 1994, Shome and Jensen, 1996, Al-Fahed et al., 1999) concluded that the heat transfer and pressure drop were not greatly affected by micro-fins. Trupp and Haine (1989) indicated that the secondary flow inside the tube with longitudinal fins was insignificant in the laminar flow and the thermal entry length was shown not to be relevant to the fin geometry.

The tube side roughening increases heat transfer surface area resulting in high efficiency heat exchangers. The increase in the surface area causes low flow rates in the heat exchanger tubes, resulting in the flow to be at Reynolds numbers that are between laminar and turbulent, that is in the transition region. Owing to the high efficiency requirements, it is likely that more HVAC units will operate in the transition region where the understandings of the heat transfer and pressure drop is limited. In the study of Esen et al. (1994) the sudden changes in the heat transfer and friction factor with Reynolds number was observed. Different tube size had different onset point of transition. Moreover, the effect of heat transfer on pressure drop is significant within the transition region. However, the end of transition was not evaluated in that study. Also, there was no further discussion on transition region in that study. Jensen and Vlakancic (1999) observed that the micro-fin tubes represented a long transitional period in friction factor before becoming fully turbulent at Re $\cong$ 20,000. During the transitional period, the friction factors are insensitive to Reynolds number. Also, this behavior was observed in Brognaux et al. (1997), Al-Fahed et al. (1999), and Chiou et al. (1995).

According to the plain tube studies done by Ghajar and Tam (1994), Tam and Ghajar (1997) and Tam and Ghajar (2006), the heat transfer and friction factor characteristics, the buoyancy effect, the entry length effect, the start and end of transition, and the effect of heating on friction factor are the important points to be considered in transition flow. However, in the past studies of micro-fin tubes, some of the above-mentioned points were always ignored. Therefore, the objective of this study is to analyze the heat transfer and friction factor characteristics of the micro-fin tubes with the above-mentioned effects taken into consideration.

EXPERIMENTAL SETUP

The heat transfer and pressure drop experimental data used in this study were obtained from the experimental apparatus shown in Figure 1. The local forced and mixed convective heat transfer measurements were made in a horizontal, electrically heated, copper circular straight tube under uniform wall heat flux boundary condition. As shown in Figure 2, two types of inlet configurations (re-entrant and square-edged) were installed before the test section. A calming and inlet section similar to that used in Ghajar and Tam (1994) was used to ensure a uniform velocity distribution at the entrance of the test section. Water and a mixture of water and ethylene glycol were used as the test fluid in the closed-loop experimental system. The DC arc welder provided the uniform heat flux boundary condition to the test section.

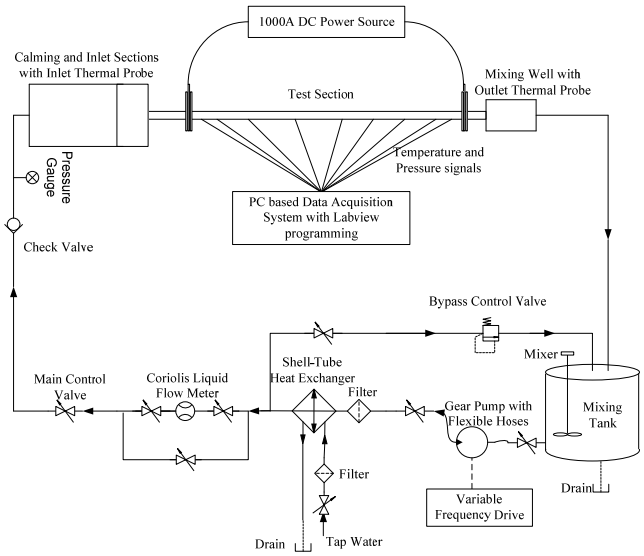

Figure 1: Experimental setup.

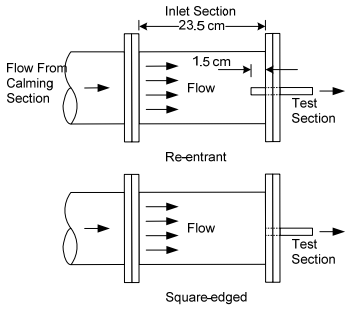

Figure 2: Type of inlet.

In this study, the plain tube and micro-fin tubes (see Figure 3) were used as the test section. Table 1 represents the specification of the tubes. The tubes have an inside diameter of 1.48 cm and an outside diameter of 1.58 cm. The total length of the test section is 6 m, providing a maximum length-to-inside diameter ratio of 403.

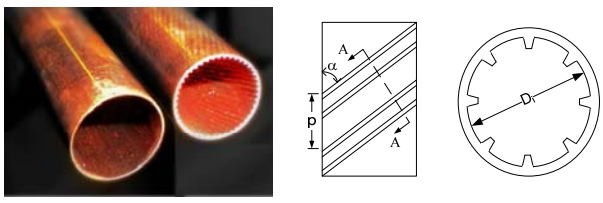

(a) (b)

Figure 3: (a) Test tubes; (b) Sectional view of the micro-fin tube.

Table 1: Specifications of the test sections

Tube Type	Tube Material	Outer Dia., D_o (mm)	Inner Dia., D_i (mm)	Spiral angle, α	Fin height, e (mm)	Number of starts, N_s
Smooth	Copper	15.88	14.88	–	–	–
Micro-fin #1	Copper	15.88	14.88	18°	0.5	25
Micro-fin #2	Copper	15.88	14.88	35°	0.5	25

As shown in Figure 4, the thermocouples denoted as TC1, TC2, TC3, and TC4, were placed 90° apart around the periphery and the single pressure tap was placed between the TC1 and TC2 thermocouples. From the local peripheral wall temperature measurements at each axial location, the inside wall temperatures and the local heat transfer coefficients were calculated by the method shown in Ghajar and Kim (2006). In these calculations, the axial conduction was assumed negligible (RePr > 4,200 in all cases), but peripheral and radial conduction of heat in the tube wall were included. In addition, the bulk fluid temperature was assumed to increase linearly from the inlet to the outlet. Also, the dimensionless numbers, such as Reynolds, Prandtl, Grashof, and Nusselt numbers were computed by the computer program developed by Ghajar and Kim (2006). In the present study, the experiments covered a local bulk Reynolds number range of 1000 to 22000, a local Prandtl number range of 5.2 to 45.3, a local bulk Grashof number range of 4496 to 23797, a local bulk Nusselt number range of 11.1 to 252.9, and a friction factor range of 7.3×10^{-3} to 2.4×10^{-2}. The wall heat flux for the experiments ranged from 3.4 to 6.9 kW/m^2.

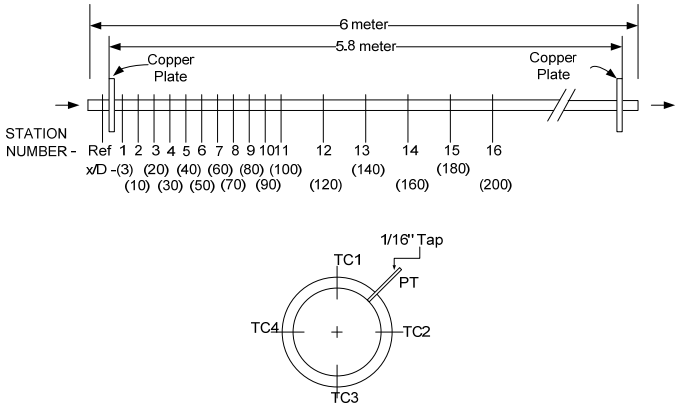

Figure 4: Arrangement of the thermocouples and pressure tap on the test section.

All the thermocouples and the pressure transducers were calibrated before the experimental runs. The high-precision Coriolis flowmeter was calibrated by the manufacturer. Table 2 lists the uncertainties of the measured variables and calculated variables over the entire range of Reynolds numbers studied. The calculation method is based on Kline and McClintock (1953).

Table 2: Uncertainies in experimental data

Measured variables		**Calculated variables**	
Variable	**Uncertainty**	**Variable**	**Uncertainty**
Temperature	0.22 °C	*C_f(friction factor)*	2.1%
Mass flow rate	0.77% of full range (0.3-30USGPM)	*h (heat transfer coefficient)*	12.6%
Density	0.2 kg/m^3	*Nu (Nusselt number)*	12.6%
Diameter	0.02mm		
Length	0.1mm		
Voltage	1%		
Current	1%		

RESULTS AND DISCUSSION

To verify the new experimental setup and later to compare with the micro-fin tube data, experiments for plain tube were conducted first. Figure 5 shows the recently collected plain tube heat transfer data for the square-edged and re-entrant inlets compared with those collected by Ghajar and Tam (1994). Since the deviations between the new data and old data were below 10%, the experimental setup and the data were confirmed to be reliable. It should be noted that the parallel shift from the classical fully developed value of Nu = 4.364 for uniform heat flux boundary condition in the laminar region is due to the buoyancy effect and it will be explained later.

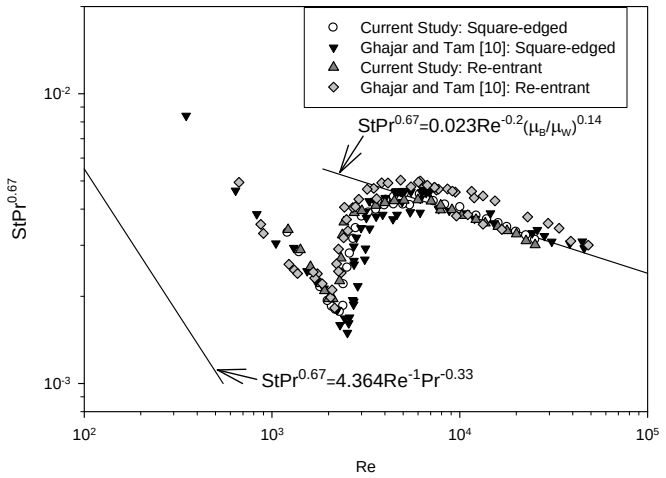

Figure 5: Heat transfer characteristics for the plain tube at x/D of 200.

The measurements of friction factor were also verified by comparing the data collected in this study with the classical friction factor equations for laminar and turbulent flows. As shown in Figure 6, all the recently collected friction factor data matched well (within 10%) with the classical equations.

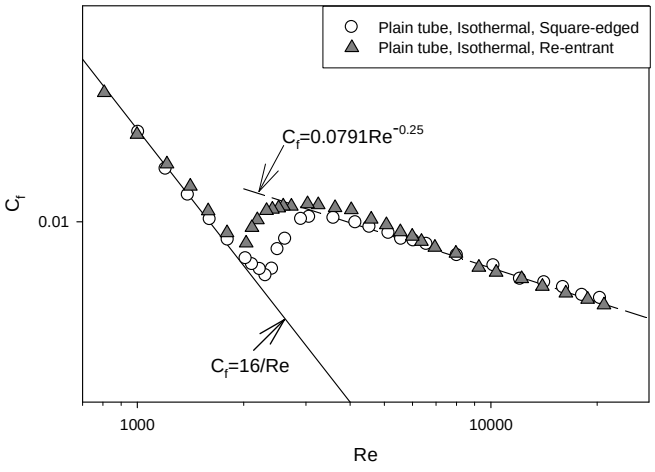

Figure 6: Friction factor characteristics for the plain tube at x/D of 200 under isothermal boundary condition.

Table 3: Start and end of transition for plain and micro-fin tubes at x/D of 200.

Tube, Condition	Heat Transfer				Friction Factor			
	Re_{start}	$StPr^{0.7}$	Re_{end}	$StPr^{0.7}$	Re_{start}	C_f	Re_{end}	C_f
Plain, Isothermal (Square-edged)	-	-	-	-	2306	7.6e-3	3588	0.0102
Plain, Heating (Square-edged)	2298	1.7e-3	8357	4.10e-3	2300	7.2e-3	3941	0.0100
Plain, Isothermal (Re-entrant)	-	-	-	-	2032	9.0e-3	3031	0.0110
Plain, Heating (Re-entrant)	2001	2.0e-3	7919	4.12e-3	2001	7.6e-3	3039	0.0106
Micro-fin #1, Isothermal (Square-edged)	-	-	-	-	2675	8.4e-3	8006	0.0144
Micro-fin #1, Heating (Square-edged)	2841	1.5e-3	9264	7.50e-3	2764	7.3e-3	8104	0.0138
Micro-fin #1, Isothermal (Re-entrant)	-	-	-	-	2021	10.4e-3	8022	0.0143
Micro-fin #1, Heating (Re-entrant)	2215	1.7e-3	8282	7.80e-3	2167	9.2e-3	7997	0.0143
Micro-fin #2, Isothermal (Square-edged)	-	-	-	-	1962	10.4e-3	7489	0.0170
Micro-fin #2, Heating (Square-edged)	2212	1.7e-3	8324	9.65e-3	2250	9.6e-3	8050	0.0168
Micro-fin #2, Isothermal (Re-entrant)	-	-	-	-	1849	11.9e-3	7989	0.0167
Micro-fin #2, Heating (Re-entrant)	1964	2e-3	8387	1.01e-2	1954	11.0e-3	7316	0.0169

After the verifications of the experimental setup, heat transfer and pressure drop data for the micro-fin tubes were measured simultaneously in a single test section. The results are shown in Figure 7 for heat transfer and Figure 8 for friction factor, respectively. As seen in these figures, the start and end of transition for heat transfer (with uniform heat flux boundary condition) and friction factor (with isothermal and uniform heat flux boundary conditions) in plain and micro-fin tubes for the two inlet configurations (square-edged and re-entrant) were established. The transition Reynolds numbers for heat transfer and friction factor are summarized in Table 3. Regarding to the start and end of transition, it can be observed, in Figure 7, that the start of transition is defined as the critical point for the sudden change from the laminar region (landed on a line parallel to Nu = 4.364) to transition region. And, the end of the transition for micro-fin tube is defined as the first point where the heat transfer data landed on a line parallel to the Sieder and Tate's correlation (1936).

As seen in Figure 4, four thermocouples were used at each location. According to Ghajar and Tam (1994, 1995), the ratio of the heat transfer coefficient of the top and bottom (h_t/h_b) should be close to unity (0.8–1.0) for forced convection and is much less than unity (< 0.8) for a case in which mixed convection exists. Ghajar and Tam (1994) established when h_t/h_b is less than 0.8, strong buoyancy effect is present. As seen in Figure 9, for the micro-fin tubes #1 and #2 with square-edged inlet when the Reynolds number is less than 2,800 and 2,200, the ratio started at one and decreased rapidly and finally stabilized when x/D was larger than 100. Recall from Table 3 that the lower transition Reynolds number for this inlet was delayed to 2,841 (for micro-fin tube #1) and to 2,212 (for micro-fin tube #2) from 2,298 for the plain tube. This delay in the transition is the direct effect of the precence of buoyancy forces in the laminar region and it is also the main reason for the parallel shift from the classical Nu value of 4.364 observed in Figures 5 and 7. No buoyancy effect was observed in the transition and turbulent regions. For the micro-fin tubes #1 and #2 with a re-entrant inlet, the buoyancy effect occurs when the Reynolds number is less than 2,300 and 2,000. As shown in Table 3, the lower transition Reynolds number for this inlet was delayed to 2,215 (for micro-fin tube #1) from 2,001 for the plain tube. However, for micro-fin tube #2, the lower transition Re was almost the same as the plain tube (1964 vs. 2001).

For the heat transfer of micro-fin tube #1, comparing with the plain tube, according to Table 3 and Figure 7, the lower transition is delayed for both square-edged and reentrant inlets. For the plain tube, the transition Reynolds number for the square-edged and re-entrant is 2298 and 2001 respectively. For micro-fin tube#1, the lower transition Reynolds number increased to 2841 for the square-edged inlet and 2215 for the re-entrant inlet. For the upper transition Reynolds number for tube#1, they were 9264 for the square-edged and 8282 for the re-entrant and therefore, the upper transition was delayed for both inlet configurations when compared with the plain tube (Re = 7919).

For the heat transfer of micro-fin tube#2, it is observed that the lower transition Reynolds number for both square-edged and re-entrant inlets were almost the same as that of the plain tube. However, for the upper transition Reynolds number, the two inlets behaved differently. For the square-edged, the upper transition Reynolds number was almost the same as the plain tube. For the re-entrant, the upper transition Reynolds number was delayed from 7919 to 8387. In this study, it can be seen that the delay of transition was more obvious for smaller spiral angle while it was not as obvious when large spiral angle tube was used. Therefore, collections of more experimental data in

the transition and turbulent regions using more micro-fin tube geometries become necessary.

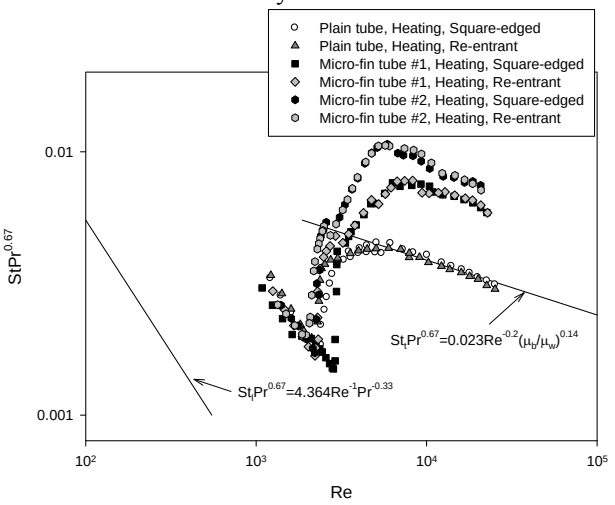

Figure 7: Heat transfer characteristics for plain and micro-fin tubes.

Referring to Figure 7, it was observed that the heat transfer behavior in the upper transition region for the plain and micro-fin tubes is very different. Around Reynolds number of 8,000 the plain tube data follows the Sieder and Tate correlation (1936) for the turbulent region. However, the micro-fin data continues to increase up to a Reynolds number of about 8,000 and then made a parallel shift from the Sieder and Tate correlation. This increase in the Colburn j factor ($St\ Pr^{0.67}$) and the parallel shift from the Sieder and Tate correlation in the turbulent region is due to the swirling motion induced by the micro-fin. The larger spiral angle (micro-fin tube #2) leads to a higher Colburn j factor. It is because the larger spiral angle increases the fluid mixing between the bulk fluid and the tube wall and therefore the heat transfer is enhanced.

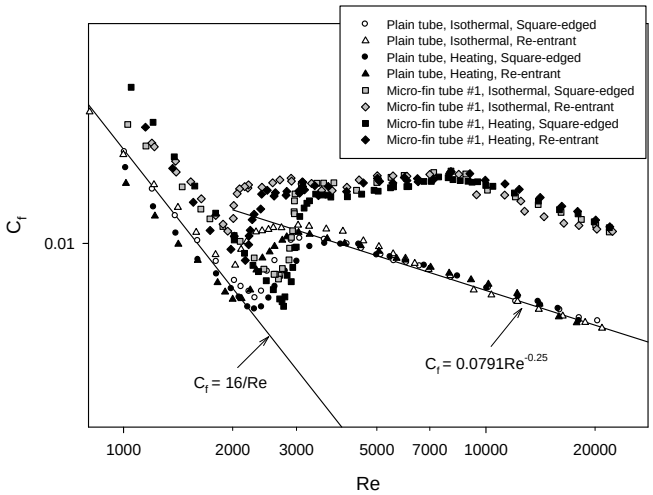

Figure 8: Friction factor characteristics for the plain and micro-fin tube #1 at x/D of 200 under isothermal and heating boundary conditions.

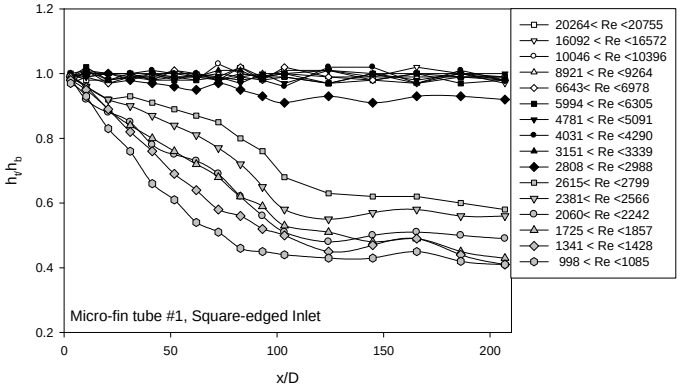

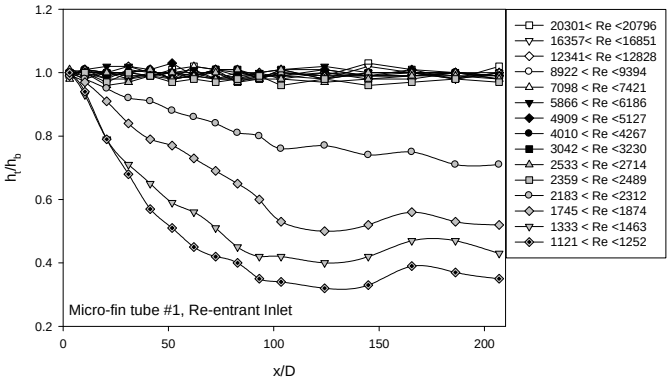

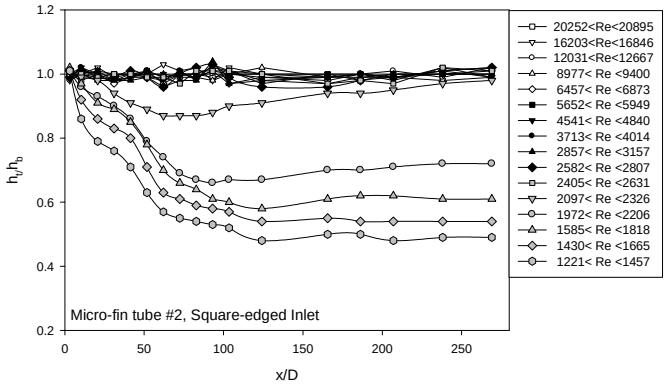

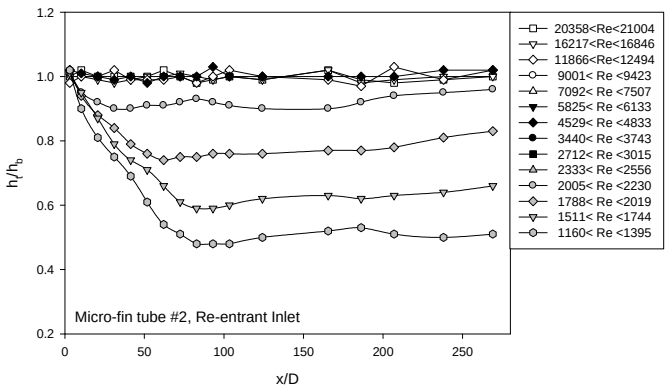

Figure 9: The ratio of heat tranfer coefficients at the top and bottom on the micro-fin tubes with different inlets.

For the friction factor, as seen in Figure 8, in the laminar region, the friction factor for micro-fin tube #1, either heated or isothermal, exhibits different behavior from the plain tube. For the micro-fin tube a parallel shift from the classical laminar equation was observed. The laminar friction factor for heated or isothermal micro-fin tube has the same trend in the laminar region. In the other words, the friction factor in that region is insensitive to the different boundary conditions. For the isothermal data, the lower transition Reynolds numbers of the micro-fin tube #1 are 2,675 and 2,021 for the square-edged and reentrant inlets which are different from the plain tube (2,306 and 2,032) and late transition for micro-fin tube was observed. Comparing the isothermal and heated friction factor for micro-fin tube, it can be observed that heating delays the start of transition. In the transition region, the friction factors go through a steep increase followed by a relatively constant C_f section and then a parallel shift from the classical Blasius turbulent friction factor correlation. Similar results were also observed in Jensen and Vlakancic (1999), Brognaux et al. (1997), Al-Fahed et al. (1999), and Chiou et al. (1995). Similar to heat transfer, it should be noted that the end of the transition for micro-fin tube is defined as the first point where the friction factor data becomes parallel to the Blasius correlation. Beyond this point, the flow is considered turbulent.

Figure 10 represents the fully developed friction factor characteristics for the different micro-fin tubes under isothermal and heating boundary conditions. The parallel shift from the classical laminar equation was also observed in the micro-fin tube #2. The laminar friction factor for the heated or isothermal micro-fin tubes has the same trend in the laminar region. In the other words, the friction factor in that region is not only insensitive to the different boundary conditions, but also insensitive to the fin geometry. For the isothermal data, the lower transition Reynolds numbers of the micro-fin tube #2 (1,962 and 1,849) for the square-edged and reentrant inlets are different from the micro-fin #1 tube (2,675 and 2,021) and early transition for micro-fin tube #2 was observed. Comparing the isothermal and heated friction factor for micro-fin tube, it can also be observed that heating delays the start of transition. In the transition region, the friction factors for the micro-fin tube #2 go through a steep increase followed by a relatively constant C_f section and then a parallel shift from the classical Blasius turbulent friction factor correlation. With a higher spiral angle in the micro-fin tube #2, the increase of friction factor can be observed in the transition and turbulent region. The reason is also caused by the mixing flow near the tube wall. As shown in Figure 10, the end of transition for both micro-fin tubes is almost the same.

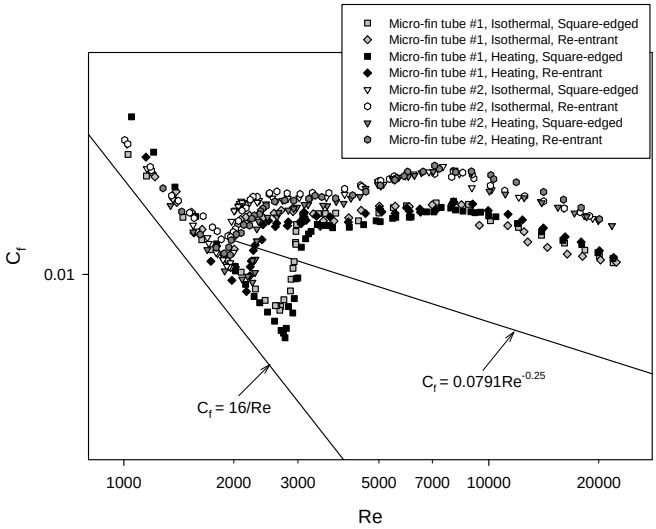

Figure 10: Friction factor characteristics for the micro-fin tubes #1 and #2 at x/D of 200 under isothermal and heating boundary conditions.

The efficiency index, $\eta = (j/C_f)_{micro-fin}/(j/C_f)_{plain}$ was calculated for the measured Reynolds number range and is plotted in Figure 11. For both micro-fin tubes #1 and #2 with two inlet types, it was observed that the efficency index is larger than one when Reynolds number is larger than 5,000. Therefore, it can be concluded that micro-fin tube should not be used in the laminar and even the lower transition regions.

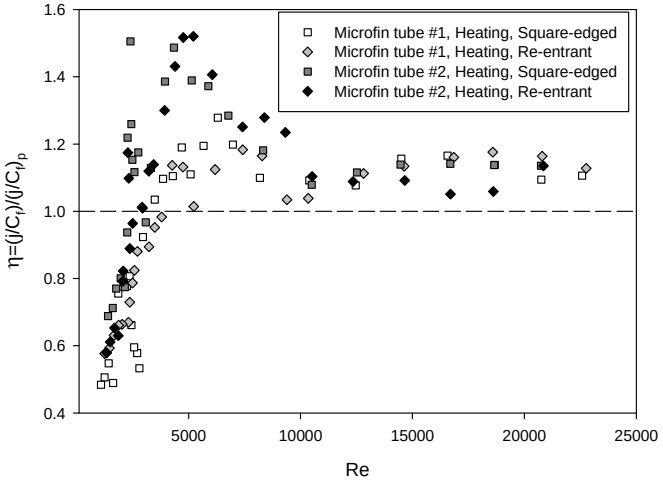

Figure 11: Efficiency index.

CONCLUSIONS

In this study, heat transfer and friction factor for horizontal plain and micro-fin tubes were obtained simultaneously under uniform wall heat flux boundary conditions. From the results, the buoyancy effect is only present in the laminar region. The transition regions for heat transfer and pressure drop were obtained. For the heat transfer, the transition is inlet dependent and the delay of transition was more obvious for smaller spiral angle while it was not as obvious when large spiral angle tube was used. In addition, a parallel shift in the heat transfer data due to the swirling motion induced by the micro-fin was observed in the turbulent region. For the micro-fin tube friction factor, a parallel shift in the laminar and turbulent regions was observed. The transition region for the friction factor is composed of a steep increase followed by a relatively constant C_f section and the results were comparable with the observations of other researchers. From the heat transfer and friction factor results, it is observed that the larger spiral angle of the micro-fin can enhance the heat transfer and pressure drop due to the occurrence of fluid mixing near the tube wall. Finally, from the calculated efficiency index values it was concluded that when the Reynolds number is larger than 5,000, regardless of the inlet configuration and fin geometry used, the efficiency index is always greater than 1.

ACKNOWLEDGMENTS

This research is supported by the Fundo para o Desenvolvimento das Ciencias e da Tecnologia under project no. 033/2008/A2 and the Institute for the Development and Quality, Macau.

NOMENCLATURE

C_f fully developed friction factor coefficient (fanning friction factor), $(=\Delta P \cdot D/2 \cdot L \cdot \rho \cdot V^2)$, dimensionless
c_p specific heat of the test fluid evaluated at T_b, J/(kg·K)
D_i inside diameter of the test section (tube), m
D_o outside diameter of the test section (tube), m
e internal fin height, mm
Gr local bulk Grashof number $[=g \cdot \beta \cdot \rho^2 \cdot D^3 (T_w - T_b) \mu^2]$, dimensionless
g acceleration of gravity, m/s^2
h fully developed peripheral heat transfer coefficient, $W/(m^2 \cdot K)$
h_b local peripheral heat transfer coefficient at the bottom of tube, $W/(m^2 \cdot K)$
h_t local peripheral heat transfer coefficient at the top of tube, $W/(m^2 \cdot K)$
j Colburn-j factor $[=St\ Pr^{0.67}]$, dimensionless
k thermal conductivity, $W/(m^2 \cdot K)$ evaluated at T_b, W/(m·K)
L length of the test section (tube), m
N_s Number of starts/fins inside the cross-section area, dimensionless
Nu local average or fully developed peripheral Nusselt number (= h·D/k), dimensionless
Pr local bulk Prandtl number $(=c_p \cdot \mu_b/k)$, dimensionless
Re local bulk Reynolds number $(=\rho \cdot V \cdot D/\mu_b)$, dimensionless
St local average or fully developed peripheral Stanton number [=Nu/(Pr·Re)], dimensionless
T_b local bulk temperature of the test fluid, ºC
T_w local inside wall temperature, ºC
V average velocity in the test section, m/s
x local axial distance along the test section from the inlet, m

Greek Symbols

α Spiral angle, degree
β coefficient of thermal expansion of the test fluid evaluated at T_b, K^{-1}
η efficiency index, dimensionless
ΔP pressure difference, Pa
μ_b absolute viscosity of the test fluid evaluated at T_b, Pa·s
μ_w absolute viscosity of the test fluid evaluated at T_w, Pa·s
ρ density of the test fluid evaluated at T_b, kg/m^3

Subscripts

plain refers to the plain tube
micro-fin refers to the micro-fin tube

REFERENCES

Al-Fahed, S., Chamra, L. M. and Chakroun, W., 1999, "Pressure drop and heat transfer comparison for both microfin tube and twisted tape inserts in laminar flow", Experimental Thermal and Fluid Science, Vol. 18, pp. 232-333.

Brognaux, L. B., Webb, R. L. and Chamra, L. M., 1997, "Single phase heat transfer in micro-fin tubes", International Journal of Heat and Mass Transfer, Vol. 40, No. 18, pp. 4345-4357.

Chiou, C. B., Wang, C. C. and Lu, D. C., 1995, "Single phase heat transfer and pressure drop characteristics of microfin tubes", ASHRAE Transactions, Vol. 101, Pt.2, pp. 1041-1048.

Esen, E. B., Obot, N. T. and Rabas, T. J., 1994, "Enhancement: Part I. Heat transfer and pressure drop results for air flow through passages with spirally-shaped roughness", Journal of Enhanced Heat Transfer, Vol. 1, No. 2, pp. 145-156.

Ghajar, A. J. and Tam, L. M., 1994, "Heat transfer measurements and correlations in the transition region for a circular tube with three different inlet configurations", Experimental Thermal and Fluid Science, Vol. 8, No. 1, pp. 79-90.

Ghajar, A. J., and Tam, L. M., 1995 "Flow regime map for a horizontal pipe with uniform wall heat flux and three inlet configurations," Experimental Thermal and Fluid Science, vol. 10, pp. 287–297.

Ghajar, A. J. and Kim, J., 2006, "Calculation of local inside-wall convective heat transfer parameters from measurements of the local outside-wall temperatures along an

electrically heated circular tube," Heat Transfer Calculations, edited by Myer Kutz, McGraw-Hill, New York, NY, pp. 23.3-23.27.

Jensen, M. K. and Vlakancic, A., 1999, "Technical note – Experimental investigation of turbulent heat transfer and fluid flow in internally finned tubes", International Journal of Heat and Mass Transfer, Vol. 42, pp. 1343-1351.

Khanpara, J. C., Bergles, A. E. and Pate, M. B., 1986, "Augmentation of R-113 in tube evaporation with microfin tubes", ASHRAE Transactions, Vol. 92, Pt. 2b, pp. 506-524.

Kline, S. J. and McClintock, F. A., 1953, "Describing Uncertainties in Single Sample Experiments," Mech. Eng., Vol. 75, No. 1, pp. 3-8.

Shome, B. and Jensen, M. K., 1996, "Experimental investigation of laminar flow and heat transfer in internally finned tubes", Journal of Enhanced Heat Transfer, Vol. 4, No. 1, pp. 53-70.

Sieder, E. N. and Tate, G. E., 1936, "Heat Transfer and Pressure Drop in Liquids in Tubes," Ind. Eng. Chem., Vol. 28, pp. 1429-1435.

Tam, L. M. and Ghajar, A. J., 1997, "Effect of inlet geometry and heating on the fully developed friction factor in the transition region of a horizontal tube", Experimental Thermal and Fluid Science, Vol. 15, No. 1, pp. 52-64.

Tam, L. M. and Ghajar, A. J., 2006, "Transitional Heat Transfer in Plain Horizontal Tubes," Heat Transfer Engineering, Vol. 27, No. 5, pp 23-38.

Trupp, A. C. and Haine, H., 1989, "Experimental investigation of turbulent mixed convection in horizontal tubes with longitudinal internal fins", National Heat Transfer Conference, Philadelphia, PA, HTD-Vol. 107, Heat Transfer in Convective Flows.

Webb, R. L., Narayanamurthy, R. and Thors, P., 2000, "Heat transfer and friction characteristics of internal helical-rib roughness", Journal of Heat Transfer, Vol. 122, No. 1, pp. 134-142.